

## Photoabsorption by Ground-State Alkali-Metal Atoms\*

Jon C. Weisheit

Harvard College Observatory, Cambridge, Massachusetts 02138

(Received 29 November 1971)

Principal-series oscillator strengths and ground-state photoionization cross sections are computed for sodium, potassium, rubidium, and cesium. The degree of polarization of the photoelectrons is also predicted for each atom. The core-polarization correction to the dipole transition moment is included in all of the calculations, and the spin-orbit perturbation of valence-*p*-electron orbitals is included in the calculations of the Rb and Cs oscillator strengths and of all the photoionization cross sections. The results are compared with recent measurements.

### I. INTRODUCTION

Applied to alkali-metal-like atoms, the Hartree-Fock approximation neglects the polarization of the core by the valence electron and treats the filled shells of the core as a spherically symmetric configuration. Bersuker,<sup>1</sup> and Hameed *et al.*<sup>2</sup> showed that the dipole moment induced in the core uniformly reduces the alkali-metal-atom principal-series oscillator strengths.

The valence-electron transitions in alkali-metal atoms are also affected by the spin-orbit interaction. The spin-orbit perturbation of valence-*p*-electron orbitals is responsible for the anomalous <sup>2</sup>*P* line-strength ratios in cesium<sup>3</sup> and for the non-zero minimum in the photoionization cross sections of ground-state Na, K, Rb, and Cs atoms.<sup>4</sup> Fano<sup>5</sup> demonstrated that it causes electrons, photoejected from alkali-metal vapors by circularly polarized light of certain wavelengths, to be strongly polarized.

In Sec. II the modification of the dipole transition moment due to core polarization and Fano's analysis of the various spin-orbit effects are reviewed, and alkali-metal valence-electron potentials are given. Computed oscillator strengths, photoionization cross sections, and spin orientation of photoelectrons are presented in Sec. III. In Sec. IV the results are discussed and compared with recent measurements.

### II. THEORY

Using stationary perturbation theory, Hameed *et al.* derived a core-polarization correction to the one-electron dipole moment for alkali-metal valence-electron transitions. In this derivation an unperturbed alkali-metal wave function is taken to be the product of a valence-electron orbital and a wave function for the undisturbed core. Neither the valence-electron Hamiltonian nor the core Hamiltonian includes the potential arising from the core-valence-electron polarization interaction. This interaction is treated as a perturbation and

then first-order corrected atomic wave functions are used to compute dipole transition moments.

The effect of the polarization interaction on the wave function of the tightly bound core electrons is small, whereas the effect on a penetrating Rydberg orbital of the valence electron can be considerable.<sup>6</sup> Consequently we outline below an alternative derivation of the core-polarization correction, in which the polarization interaction is treated as a perturbation of the core wave function but is included in the valence-electron eigenvalue equation which is solved numerically. This approach is based on the derivation by Caves and Dalgarno<sup>7</sup> and leads to the result given by Bersuker. Atomic units are used throughout.

In a manner analogous to the Born-Oppenheimer treatment of diatomic molecules, we make the approximation that the *N* core electrons, located at  $\vec{r}_j$  ( $j = 1, 2, \dots, N$ ), respond instantaneously to the (relatively slow) changes in position of the valence electron, located at  $\vec{r}$ . Then, if exchange between the valence electron and core electrons is neglected, the (*N*+1)-electron wave function may be written in a parameterized form,

$$\Psi_\alpha(\vec{r}_j, \vec{r}) = \chi_0(\vec{r}_j | \vec{r}) \psi_\alpha(\vec{r}), \quad (1)$$

where  $\chi_0$  is the ground-state core wave function and  $\psi_\alpha$  is the orbital of the valence electron.

The total electrostatic Hamiltonian *H* is conveniently separated in three parts,

$$H = H_c + T_r + H_i, \quad (2)$$

where the *N*-electron core Hamiltonian is  $H_c$ , the valence electron's kinetic-energy operator is  $T_r = -\frac{1}{2} \nabla_r^2$ , the electrostatic interaction Hamiltonian is

$$H_i = -\frac{Z}{r} + \sum_{j=1}^N |\vec{r}_j - \vec{r}|^{-1}, \quad (3)$$

and the nuclear charge is *Z*. An unperturbed core wave function  $\chi_t(\vec{r}_j | \infty) = \chi_t^{(0)}$  is an eigenfunction of  $H_c$  with eigenvalue  $E_t^{(0)}$ .

The substitution of the wave function (1), with

$\vec{r}$  held constant, into the Schrödinger equation yields the eigenvalue equation for  $\chi_0$ ,

$$[H_c + H_i - V(r) - E_0^{(0)}] \chi_0(\vec{r}_j | \vec{r}) = 0, \quad (4)$$

where  $[V(r) + E_0^{(0)}]$  is the  $r$ -dependent eigenvalue. The eigenvalue equation for  $\psi_\alpha$  is then readily obtained,

$$[T_r + V(r) - \epsilon_\alpha] \psi_\alpha(\vec{r}) = \mathcal{C}_0(\vec{r}) \psi_\alpha(\vec{r}). \quad (5)$$

In Eq. (5),  $\epsilon_\alpha$  is the valence-electron eigenvalue and  $\mathcal{C}_0(\vec{r}) = \langle \chi_0 | T_r | \chi_0 \rangle$  is the adiabatic coupling term<sup>8</sup> which, in the present case, behaves asymptotically as  $r^{-6}$ .

If the interaction Hamiltonian  $H_i$  in Eq. (4) is treated as a perturbation of the core wave function  $\chi_0^{(0)}$ , it follows that

$$\chi_0(\vec{r}_j | \vec{r}) \approx \chi_0^{(0)}(\vec{r}_j | \infty) + \chi_0^{(1)}(\vec{r}_j | \vec{r}), \quad (6)$$

where the first-order correction is given by the familiar expression

$$\chi_0^{(1)}(\vec{r}_j | \vec{r}) = - \sum'_{t \neq 0} \chi_t^{(0)} \langle \chi_t^{(0)} | H_i | \chi_0^{(0)} \rangle (E_t^{(0)} - E_0^{(0)})^{-1}. \quad (7)$$

$\sum'$  indicates that discrete and continuum core states are included in the summation.

Through first order the potential-energy term in Eqs. (4) and (5) is

$$V(r) = \langle \chi_0^{(0)} | H_i | \chi_0^{(0)} \rangle + \langle \chi_0^{(0)} | H_i | \chi_0^{(1)} \rangle. \quad (8)$$

This potential has the asymptotic behavior

$$V(r) \sim N r^{-1} - \frac{1}{2} \alpha_d r^{-4} - \frac{1}{2} \alpha_q r^{-6}, \quad (9)$$

where  $\alpha_d$  and  $\alpha_q$  are the static dipole and quadrupole core polarizabilities, so by solving the eigenvalue equation (5) directly we include the full effect of the polarization interaction on the valence electron. As we show below, to a good approximation the perturbation of the core wave function can be treated analytically.

The dipole moment for the valence-electron transition  $\alpha \rightarrow \beta$  is defined as

$$\vec{M}_{\beta\alpha} = \langle \psi_\beta | \vec{d} + \vec{D} | \psi_\alpha \rangle, \quad (10)$$

where  $\vec{d} = -\vec{r}$  and  $\vec{D} = -\sum_j \vec{r}_j$  are the valence- and core-electron dipole operators, respectively. Using Eqs. (1) and (6), through first order this becomes

$$\vec{M}_{\beta\alpha} = \langle \psi_\beta | \vec{Q}(\vec{r}) | \psi_\alpha \rangle, \quad (11)$$

where the "effective" dipole operator is

$$\vec{Q}(\vec{r}) = \langle \chi_0^{(0)} | \vec{d} + \vec{D} | \chi_0^{(0)} \rangle + \langle \chi_0^{(1)} | \vec{d} + \vec{D} | \chi_0^{(0)} \rangle + \langle \chi_0^{(0)} | \vec{d} + \vec{D} | \chi_0^{(1)} \rangle. \quad (12)$$

To reduce  $\vec{Q}$  to a tractable form, we take advantage of the fact that the valence electron is localized outside the core, and expand  $H_i$  in a power series

of  $r$ . The first term that gives a nonvanishing contribution in Eq. (7) is the dipole term,

$$H_i(\text{dipole}) = \sum_{j=1}^N \frac{r_j}{r^2} P_1(\vec{r}_j \cdot \vec{r}) = \frac{\vec{D} \cdot \vec{d}}{r^3}. \quad (13)$$

The replacement of  $H_i$  in Eq. (7) by this one term leads to the result

$$\vec{Q}(\vec{r}) = \vec{d} \left( 1 - 2r^{-3} \sum'_{t=0} \frac{|\langle \chi_t^{(0)} | \vec{D} | \chi_0^{(0)} \rangle|^2}{E_t^{(0)} - E_0^{(0)}} \right) = -\vec{r} \left( 1 - \alpha_d \frac{\alpha_d}{r^3} \right). \quad (14)$$

The derivation by Hameed *et al.* yields Eq. (14), but with  $\alpha_d$  replaced by  $\alpha_d(\omega)$ , the dynamic polarizability of the core at the transition frequency  $\omega$ . However, "unpolarized" valence-electron orbitals, that is, orbitals which are eigenfunctions of the one-electron Hamiltonian that *does not* include polarization interaction terms, are then used in Eq. (11) to compute the dipole moment  $\vec{M}$ . (Norcross<sup>9</sup> has pointed out that in Hameed's derivation, the use of "polarized" valence-electron orbitals leads to additional complicated terms in the expression for  $\vec{Q}$ .) The correct expression for  $\vec{Q}$  at all  $r$  values can only be written down formally [Eq. (12)], so in either case Eq. (14) must be modified such that  $\vec{Q}$  remains finite at the origin. This necessary, but essentially arbitrary, modification of  $\vec{Q}$  makes differences between Hameed's treatment of core polarization and the treatment of Caves and Dalgarno difficult to assess quantitatively, though the Born-Oppenheimer approach, which utilizes "polarized" valence-electron orbitals, seems physically more plausible.

We have used the form

$$\vec{Q} = -\vec{r} \{ 1 - \alpha_d r^{-3} [1 - \exp(-(r/r_0)^3)] \}, \quad (15)$$

where  $r_0$  is an effective core-radius cutoff. Dalgarno and the author have discussed the sensitivity of computed dipole transition moments with respect to different  $r_0$  values and different forms of the modification of  $\vec{Q}$ , and have shown that, for a given form of the modified operator  $\vec{Q}$ , one value of  $r_0$  may be used to reproduce a variety of experimental measurements.<sup>10,11</sup> The manner in which  $r_0$  values were determined for the present calculations is discussed at the end of this section.

The iterative perturbation procedure described by Bottcher<sup>12</sup> has been employed to obtain model potentials of the form

$$V_m(r) = V_c(r) - \frac{1}{2} \alpha_d r^{-4} \{ 1 - \exp[-(r/r_1)^6] \} - \frac{1}{2} \lambda r^{-6} \{ 1 - \exp[-(r/r_1)^8] \} + (c_1 + c_2 r) \exp(-r/r_0) \quad (16)$$

for the valence electron of Na, K, Rb, and Cs.  $V_c$  is the core potential, computed from Clementi's<sup>13</sup>

TABLE I. Core radius  $r_c$  in the effective dipole operator [Eq. (15)] and parameters for the alkali-metal valence-electron potential [Eqs. (16) and (17)]. All values are in atomic units.

|            | Na                  | K                  | Rb                 | Cs                 |
|------------|---------------------|--------------------|--------------------|--------------------|
| $r_c$      | 2.350               | 4.220              | 3.505              | 4.834              |
| $\alpha_d$ | 0.9459 <sup>a</sup> | 5.331 <sup>b</sup> | 8.976 <sup>c</sup> | 19.06 <sup>d</sup> |
| $\lambda$  | 6.9273              | 4.1026             | 113.18             | 581.60             |
| $c_1$      | 0.38514             | 1.0793             | -0.97872           | -0.79710           |
| $c_2$      | -0.10506            | 0.34470            | 0.16158            | 0.15052            |
| $r_0$      | 1.00                | 1.20               | 1.40               | 1.50               |
| $r_1$      | 1.00                | 1.20               | 3.75               | 4.00               |
| $(Z-a)$    | 12.48               | 17.33              | 26.70              | 39.77              |

<sup>a</sup>J. Lahiri and A. Mukherji, Phys. Rev. **153**, 386 (1967).

<sup>b</sup>J. Lahiri and A. Mukherji, Phys. Rev. **155**, 24 (1967).

<sup>c</sup>I. Johansson, Arkiv Fysik **20**, 135 (1961).

<sup>d</sup>J. Heinrichs, J. Chem. Phys. **52**, 6316 (1970).

data for Na and K, and from Hartree's<sup>14</sup> data for Rb and Cs; the nonlinear parameters  $r_0$  and  $r_1$  are chosen *ab initio* and the linear parameters  $\lambda$ ,  $c_1$ , and  $c_2$  are then determined numerically from the observed alkali spectra. By not requiring that  $\lambda = \alpha_d$  in Eq. (16), we can effectively include the long-range contribution from the adiabatic coupling term  $\mathcal{C}_0(\vec{r})$  in the valence-electron model potential. Values of the parameters in Eq. (16) have previously been reported for sodium and potassium,<sup>10</sup> but for completeness these are listed in Table I with the parameters for the cesium and rubidium model potentials. It is interesting to note that the Cs model potential is very similar to the unusual numerical potential constructed by Stone that reproduces cesium eigenvalues.<sup>15</sup>

The tabulated model potential parameters are obtained by neglecting the spin-orbit splitting and

matching computed eigenvalues to values of the measured center of gravity of each of several terms. The spin-orbit interaction  $V_{so}(r)$  has been included in the total valence-electron potential  $V(r)$  by means of the ansatz

$$V(r) = V_m(r) + V_{so}(r) \\ = V_m(r) + \frac{1}{2}\alpha^2 \vec{l} \cdot \vec{s}(Z-a)/r^3, \quad (17)$$

where  $\alpha$  is the fine-structure constant,  $\vec{l}$  and  $\vec{s}$  are the orbital and spin angular momenta of the valence electron, and  $a$  is a screening constant. For each atom, the value of  $(Z-a)$  listed in Table I was determined from measured  $n^2P$  fine-structure energy defects  $\Delta\epsilon_n$  by averaging several computed values of

$$(Z-a_n) = \Delta\epsilon_n \left( \frac{3}{4} \alpha^2 \langle \psi_{np} | r^{-3} | \psi_{np} \rangle \right)^{-1}.$$

To illustrate the accuracy of the valence-electron potentials, computed and experimental Cs eigenvalues are compared in Table II; computed values of  $(Z-a_n)$  are given also. For increasing  $n$ , the  $(Z-a_n)$  converge rapidly to values near the tabulated average.

The effects of the spin-orbit interaction on radiative transitions from an alkali-metal ground state may be described conveniently in terms of the parameter  $x$ , introduced by Fano,<sup>5</sup>

$$x = (2M_3 + M_1)/(M_3 - M_1), \quad (18)$$

where  $M_3$  and  $M_1$  are the radial parts of dipole moments for transitions to  $(j = \frac{3}{2})$  and  $(j = \frac{1}{2})$  final  $p$  states, respectively,

$$M_{3(1)} = \langle \text{ground state} | Q(r) | \text{final state}; j = \frac{3}{2}(\frac{1}{2}) \rangle. \quad (19)$$

Below the ionization threshold, the parameter  $x$  is defined only at the discrete valence-electron

TABLE II. Cesium eigenvalues<sup>a</sup> (rydbergs) and computed values of  $(Z-a_n)$ .

| $n$ | $^2P_{1/2}$              |             | $^2P_{3/2}$ |             | $(Z-a_n)$           |
|-----|--------------------------|-------------|-------------|-------------|---------------------|
|     | Observed                 | Computed    | Observed    | Computed    |                     |
| 6   | -1.8434(-1) <sup>b</sup> | -1.8532(-1) | -1.7929(-1) | -1.7906(-1) | 33.862 <sup>c</sup> |
| 7   | -8.7858(-2)              | -8.8027(-2) | -8.6208(-2) | -8.6206(-2) | 37.730              |
| 8   | -5.1922(-2)              | -5.1953(-2) | -5.1168(-2) | -5.1150(-2) | 38.984              |
| 9   | -3.4348(-2)              | -3.4356(-2) | -3.3940(-2) | -3.3929(-2) | 39.536              |
| 10  | -2.4417(-2)              | -2.4419(-2) | -2.4172(-2) | -2.4164(-2) | 39.814              |
| 11  | -1.8253(-2)              | -1.8252(-2) | -1.8094(-2) | -1.8087(-2) | 40.069              |
| 12  | -1.4160(-2)              | -1.4160(-2) | -1.4052(-2) | -1.4048(-2) | 40.001              |
| 13  | -1.1306(-2)              | -1.1305(-2) | -1.1229(-2) | -1.1226(-2) | 40.215              |
| 14  | -9.2362(-3)              | -9.2352(-3) | -9.1786(-3) | -9.1762(-3) | 40.521              |
| 15  | -7.6861(-3)              | -7.6859(-3) | -7.6431(-3) | -7.6411(-3) | 39.729              |
| 16  | -6.4969(-3)              | -6.4962(-3) | -6.4627(-3) | -6.4615(-3) | 40.857              |
| 17  | -5.5634(-3)              | -5.5632(-3) | -5.5365(-3) | -5.5356(-3) | 40.389              |
| 18  | -4.8174(-3)              | -4.8304(-3) | -4.7960(-3) | -4.8100(-3) | 39.403              |

<sup>a</sup>The computed Cs ( $6s_{1/2}$ ) eigenvalue is  $-0.28583$  Ry and the observed value is  $-0.28620$  Ry.

<sup>b</sup>The notation is  $-1.8434(-1) = -1.8434 \times 10^{-1}$ .

<sup>c</sup>This entry was excluded in the determination of the average value  $(Z-a)$ .

TABLE III. The total cross section  $\sigma_T$  and Fano parameter  $x$  for the photoionization of ground-state sodium atoms. The incident photon's energy  $E$  and wavelength  $\lambda$  are both indicated.

| $E$ (eV) | $\lambda$ (Å) | $\sigma_T$ ( $10^{-18}$ cm $^2$ ) | $x$        |
|----------|---------------|-----------------------------------|------------|
| 5.140    | 2409          | 1.198(-1)                         | 1.179(+2)  |
| 5.161    | 2400          | 1.142(-1)                         | 1.155(+2)  |
| 5.275    | 2348          | 8.631(-2)                         | 1.024(+2)  |
| 5.445    | 2275          | 5.473(-2)                         | 8.380(+1)  |
| 5.683    | 2180          | 2.570(-2)                         | 5.958(+1)  |
| 5.989    | 2068          | 6.432(-3)                         | 3.117(+1)  |
| 6.131    | 2020          | 2.295(-3)                         | 1.896(+1)  |
| 6.283    | 1972          | 2.624(-4)                         | 6.414(+0)  |
| 6.363    | 1947          | 1.191(-5)                         | 3.782(-2)  |
| 6.446    | 1922          | 2.494(-4)                         | -6.392(+0) |
| 6.620    | 1871          | 2.097(-3)                         | -1.938(+1) |
| 6.805    | 1820          | 5.594(-3)                         | -3.246(+1) |
| 7.316    | 1694          | 1.988(-2)                         | -6.520(+1) |
| 7.894    | 1570          | 3.879(-2)                         | -9.730(+1) |
| 8.540    | 1451          | 5.867(-2)                         | -1.281(+2) |
| 10.04    | 1235          | 9.173(-2)                         | -1.844(+2) |
| 11.81    | 1050          | 1.099(-1)                         | -2.327(+2) |
| 13.85    | 895           | 1.144(-1)                         | -2.732(+2) |

eigenenergies, but  $x$  behaves smoothly as it passes through the ionization threshold and is then a continuous function of the photoejected-electron momentum  $k$  or, equivalently, of the ionizing photon energy  $E$ .

Both the  $^2P$  line-strength ratio  $\rho$  and the degree of spin orientation of electrons photoejected by circularly polarized light  $P$  may be expressed in terms of  $x$ , viz.,

$$\rho = (f_3/f_1) (\epsilon_1/\epsilon_3) = 2(x+1)^2/(x-2)^2 \quad (20)$$

and

$$P = (2x+1)/(x^2+2), \quad (21)$$

where, in Eq. (20),  $f_3$  and  $f_1$  are oscillator strengths for transitions to  $(j = \frac{3}{2})$  and  $(j = \frac{1}{2})$   $^2P$  levels with eigenvalues  $\epsilon_3$  and  $\epsilon_1$ . In addition, the total photoionization cross section  $\sigma_T$ , which is obtained by summing contributions to degenerate  $(j = \frac{1}{2})$  and  $(j = \frac{3}{2})$  continuum levels, and the photoionization cross section  $\sigma_*$ , obtained by neglecting the spin-orbit perturbation, are related by the equation

$$(\sigma_*/\sigma_T) = x^2/(x^2+2). \quad (22)$$

Equations (20)–(22) are only approximately correct because nuclear spin effects and the difference between  $(j = \frac{1}{2})$  and  $(j = \frac{3}{2})$  valence-orbital phase shifts are neglected in the definition of  $x$ , Eq. (18). However, Fano has shown that the resultant modifications of the definition of  $x$  are quite small, so they will not be considered in this investigation.

Prompted by Fano's suggestion that, because of the spin-orbit interaction, photoionization of alkali metal vapors might provide a usable source

TABLE IV. Same as Table III, for potassium.

| $E$ (eV) | $\lambda$ (Å) | $\sigma_T$ ( $10^{-18}$ cm $^2$ ) | $x$        |
|----------|---------------|-----------------------------------|------------|
| 4.342    | 2855          | 6.007(-3)                         | 6.640(+0)  |
| 4.353    | 2848          | 5.375(-3)                         | 6.281(+0)  |
| 4.374    | 2834          | 4.235(-3)                         | 5.567(+0)  |
| 4.407    | 2813          | 2.820(-3)                         | 4.509(+0)  |
| 4.451    | 2786          | 1.459(-3)                         | 3.118(+0)  |
| 4.505    | 2752          | 4.829(-4)                         | 1.414(+0)  |
| 4.536    | 2733          | 2.623(-4)                         | 4.496(-1)  |
| 4.570    | 2713          | 2.745(-4)                         | -5.849(-1) |
| 4.607    | 2691          | 5.586(-4)                         | -1.687(-1) |
| 4.647    | 2668          | 1.149(-3)                         | -2.854(+0) |
| 4.689    | 2644          | 2.076(-3)                         | -4.082(+0) |
| 4.734    | 2619          | 3.360(-3)                         | -5.367(+0) |
| 4.781    | 2593          | 5.020(-3)                         | -6.708(+0) |
| 4.832    | 2566          | 7.068(-3)                         | -8.099(+0) |
| 4.885    | 2538          | 9.506(-3)                         | -9.538(+0) |
| 4.940    | 2509          | 1.233(-2)                         | -1.102(+1) |
| 5.060    | 2450          | 1.911(-2)                         | -1.411(+1) |
| 5.191    | 2388          | 2.728(-2)                         | -1.733(+1) |
| 5.565    | 2228          | 5.222(-2)                         | -2.580(+1) |
| 6.517    | 1902          | 1.064(-1)                         | -4.338(+1) |
| 7.742    | 1601          | 1.430(-1)                         | -5.996(+1) |
| 9.230    | 1342          | 1.536(-1)                         | -7.449(+1) |
| 11.01    | 1126          | 1.452(-1)                         | -8.657(+1) |

of polarized electrons, Baum *et al.*<sup>16</sup> have measured  $x(E)$  for K, Rb, and Cs, and Kessler and co-workers<sup>17</sup> have independently measured  $x(E)$  for Cs. Their experiments have accurately determined the zero of  $x(E)$  for these atoms, which occurs near the photoionization cross-section minimum. These

TABLE V. Same as Table III, for rubidium.

| $E$ (eV) | $\lambda$ (Å) | $\sigma_T$ ( $10^{-18}$ cm $^2$ ) | $x$        |
|----------|---------------|-----------------------------------|------------|
| 4.176    | 2967          | 8.903(-2)                         | 5.318(+0)  |
| 4.208    | 2944          | 8.009(-2)                         | 5.069(+0)  |
| 4.251    | 2915          | 6.939(-2)                         | 4.749(+0)  |
| 4.311    | 2875          | 5.636(-2)                         | 4.308(+0)  |
| 4.387    | 2824          | 4.243(-2)                         | 3.754(+0)  |
| 4.481    | 2765          | 2.914(-2)                         | 3.095(+0)  |
| 4.568    | 2713          | 1.987(-2)                         | 2.497(+0)  |
| 4.666    | 2656          | 1.242(-2)                         | 1.843(+0)  |
| 4.774    | 2595          | 7.207(-3)                         | 1.137(+0)  |
| 4.894    | 2532          | 4.451(-3)                         | 3.856(-1)  |
| 4.926    | 2516          | 4.159(-3)                         | 1.911(-1)  |
| 4.958    | 2499          | 4.046(-3)                         | -5.825(-3) |
| 4.991    | 2483          | 4.051(-3)                         | -2.053(-1) |
| 5.025    | 2466          | 4.232(-3)                         | -4.070(-1) |
| 5.166    | 2399          | 6.480(-3)                         | -1.236(+0) |
| 5.319    | 2330          | 1.101(-2)                         | -2.096(+0) |
| 5.482    | 2261          | 1.754(-2)                         | -2.982(+0) |
| 5.656    | 2191          | 2.572(-2)                         | -3.892(+0) |
| 5.841    | 2122          | 3.521(-2)                         | -4.820(+0) |
| 6.351    | 1951          | 6.217(-2)                         | -7.196(+0) |
| 7.576    | 1636          | 1.137(-1)                         | -1.206(+1) |
| 9.072    | 1366          | 1.443(-1)                         | -1.687(+1) |
| 10.84    | 1143          | 1.515(-1)                         | -2.148(+1) |

TABLE VI. Same as Table III, for cesium.

| $E$ (eV) | $\lambda$ (Å) | $\sigma_T$ ( $10^{-18}$ cm $^2$ ) | $x$        |
|----------|---------------|-----------------------------------|------------|
| 3.890    | 3183          | 1.003(-1)                         | 1.772(+0)  |
| 3.923    | 3156          | 9.172(-2)                         | 1.671(+0)  |
| 3.965    | 3123          | 8.158(-2)                         | 1.541(+0)  |
| 4.025    | 3077          | 6.936(-2)                         | 1.362(+0)  |
| 4.101    | 3019          | 5.671(-2)                         | 1.137(+0)  |
| 4.195    | 2952          | 4.500(-2)                         | 8.693(-1)  |
| 4.305    | 2876          | 3.557(-2)                         | 5.626(-1)  |
| 4.433    | 2794          | 2.936(-2)                         | 2.211(-1)  |
| 4.461    | 2776          | 2.856(-2)                         | 1.490(-1)  |
| 4.489    | 2759          | 2.790(-2)                         | 7.572(-2)  |
| 4.518    | 2741          | 2.741(-2)                         | 1.288(-3)  |
| 4.547    | 2723          | 2.705(-2)                         | -7.428(-2) |
| 4.578    | 2705          | 2.686(-2)                         | -1.509(-1) |
| 4.608    | 2687          | 2.682(-2)                         | -2.286(-1) |
| 4.640    | 2669          | 2.693(-2)                         | -3.074(-1) |
| 4.672    | 2651          | 2.735(-2)                         | -3.870(-1) |
| 4.739    | 2613          | 2.814(-2)                         | -5.493(-1) |
| 4.808    | 2576          | 2.966(-2)                         | -7.151(-1) |
| 4.955    | 2499          | 3.424(-2)                         | -1.056(+0) |
| 5.113    | 2422          | 4.061(-2)                         | -1.409(+0) |
| 5.555    | 2230          | 6.185(-2)                         | -2.326(+0) |
| 6.066    | 2042          | 8.580(-2)                         | -3.274(+0) |
| 7.290    | 1699          | 1.238(-1)                         | -5.178(+0) |
| 8.786    | 1410          | 1.366(-1)                         | -6.974(+0) |
| 10.56    | 1174          | 1.287(-1)                         | -8.568(+0) |

measurements provide the most precise determination of the cutoff parameter  $r_c$  in the effective-dipole operator  $\tilde{Q}$ . The values of  $r_c$  listed in Table I reproduce the zero point of  $x$  for potassium and for rubidium as measured by Baum *et al.* and the average measured zero point of  $x$  for cesium. For sodium,  $r_c$  was determined from the measured photoionization cross section at threshold.<sup>18</sup> These  $r_c$  values are used in all of the calculations presented in Sec. III.

TABLE VII. Oscillator strengths for alkali-metal-atom principal-series transitions  $n_0$   $^2S - n$   $^2P$ .  $f_*$  indicates the oscillator strength computed neglecting the spin-orbit perturbation of  $p$  orbitals;  $f_{1(3)}$  indicates the oscillator strength for the transitions to the  $j = \frac{1}{2}(\frac{3}{2})$  level of the  $^2P$  state.

| $(n - n_0)$ | Sodium    | Potassium | Rubidium  |           | Cesium     |           |
|-------------|-----------|-----------|-----------|-----------|------------|-----------|
|             | $f_*$     | $f_*$     | $f_1$     | $f_3$     | $f_1$      | $f_3$     |
| 0           | 9.694(-1) | 9.732(-1) | 3.499(-1) | 7.114(-1) | 3.538(-1)  | 7.404(-1) |
| 1           | 1.376(-2) | 8.377(-3) | 3.473(-3) | 9.580(-3) | 2.035(-3)  | 1.050(-2) |
| 2           | 2.099(-3) | 8.230(-4) | 4.278(-4) | 1.442(-3) | 1.555(-4)  | 1.639(-3) |
| 3           | 6.478(-4) | 1.776(-4) | 1.117(-4) | 4.396(-4) | 2.429(-5)  | 5.120(-4) |
| 4           | 2.801(-4) | 5.742(-5) | 4.238(-5) | 1.878(-4) | 5.318(-6)  | 2.231(-4) |
| 5           | 1.468(-4) | 2.383(-5) | 2.011(-5) | 9.755(-5) | 1.394(-6)  | 1.171(-4) |
| 6           | 8.705(-5) | 1.170(-5) | 1.112(-5) | 5.777(-5) | 3.989(-7)  | 6.886(-5) |
| 7           | 5.612(-5) | 6.460(-6) | 6.848(-6) | 3.740(-5) | 1.100(-7)  | 4.485(-5) |
| 8           | 3.846(-5) | 3.924(-6) | 4.426(-6) | 2.508(-5) | 2.626(-8)  | 3.067(-5) |
| 9           | 2.759(-5) | 2.547(-6) | 3.022(-6) | 1.794(-5) | 5.151(-9)  | 2.209(-5) |
| 10          | 2.011(-5) | 1.718(-6) | 2.182(-6) | 1.331(-5) | 1.623(-10) | 1.609(-5) |
| 11          | 1.570(-5) | 1.249(-6) | 1.634(-6) | 1.020(-5) | 4.083(-10) | 1.263(-5) |
| 12          | 1.178(-5) | 9.138(-7) | 1.261(-6) | 7.990(-6) | 2.155(-9)  | 1.001(-5) |

### III. COMPUTATIONS

Bound and continuum orbitals have been obtained from the numerical solution of the valence-electron eigenvalue equation

$$(T_r + V_m + V_{so} - \epsilon_\alpha)\psi_\alpha = 0. \quad (23)$$

The spin-orbit interaction  $V_{so}$  was not included in the determination of *bound-p*-state orbitals for sodium and potassium since the observed  $^2P$  line-strength ratio is approximately 2 for all principal-series transitions of these atoms.

Tables III–VI list the total photoionization cross section  $\sigma_T$  and Fano parameter  $x$  computed for sodium, potassium, rubidium, and cesium. The effect of the spin-orbit interaction on each photoionization cross section can be found easily from these tables by using Eq. (22). Some of the potassium results have been reported previously,<sup>11</sup> but are presented again for the sake of completeness.

Sodium and potassium principal-series oscillator strengths  $f_*$ , computed by neglecting the spin-orbit interaction, and rubidium and cesium principal-series oscillator strengths  $f_1$  and  $f_3$  are listed in Table VII. The sodium  $f$  values have been reported already,<sup>10</sup> but the other  $f$  values are new, having been computed with the accurately determined value of the core radius  $r_c$  for each atom.

In Sec. IV these numerical results are discussed, and comparisons with recent measurements are made.

### IV. DISCUSSION

(a) *Sodium*. The computed sodium photoionization cross section  $\sigma_T$  is compared with the cross section measured by Hudson and Carter<sup>19</sup> in Fig. 1. Both the computed value of the cross section at its minimum  $\sigma_{min}$  and the computed position of the minimum  $\lambda_{min}$  are given in Table VIII, which also in-

TABLE VIII. Alkali-metal-atom ground-state photoionization-cross-section minima. The tabulated cross sections are in units  $10^{-20} \text{ cm}^2$  and the tabulated wavelengths in  $\text{\AA}$ .

|    | Present work          |                        | Seaton<br>(Ref. 4)    | Experimental                   |  |
|----|-----------------------|------------------------|-----------------------|--------------------------------|--|
|    | $\sigma_{\text{min}}$ | $\lambda_{\text{min}}$ | $\sigma_{\text{min}}$ | $\sigma_{\text{min}}$          | $\lambda_{\text{min}}$                               |
| Na | 0.0009                | 1940                   | 0.001                 | $< 0.3$<br>$< 0.1$             | $1920 \pm 30^{\text{a}}$<br>$1950 \pm 50^{\text{b}}$ |
| K  | 0.022                 | 2720                   | 0.03                  | $0.4 \pm 0.2$<br>$0.2 \pm 0.2$ | $2725 \pm 15^{\text{a}}$<br>$2675 \pm 75^{\text{c}}$ |
| Rb | 0.40                  | 2500                   | 0.4                   | $0.8 \pm 0.3$                  | $2480 \pm 25^{\text{a}}$                             |
| Cs | 2.68                  | 2685                   | 3.0                   | $6 \pm 1$                      | $2650 \pm 25^{\text{a}}$                             |

<sup>a</sup>Marr and Creek, Ref. 18.

<sup>b</sup>Hudson and Carter, Ref. 19.

<sup>c</sup>Hudson and Carter, Ref. 20.

cludes an estimate by Seaton and the measured values of these quantities. The agreement among the different entries is very good. As with all previously reported calculations (see Ref. 18 for a compilation), the present cross section does not rise as steeply on the short-wavelength side of the minimum as the experimentally determined cross section does. The reason for this persistent discrepancy has not been established yet.

Because the spin-orbit perturbation of Na orbitals is small,  $\chi(E)$  is large except very near the cross-section minimum. Consequently, no measurements of  $\chi$  have been made for sodium.

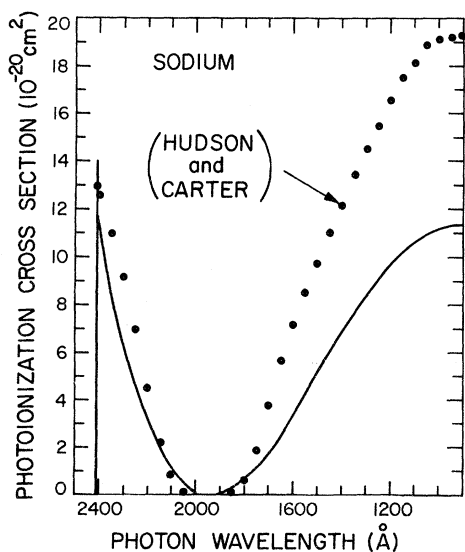


FIG. 1. Sodium photoionization cross section. The curve indicates results obtained by including both the spin-orbit interaction and the core-polarization correction to the dipole transition moment. The filled circles are measurements reported by Hudson and Carter, Ref. 19.

The computed sodium oscillator strengths are in accord with those predicted by Marr and Creek,<sup>21</sup> and with those suggested by Dalgarno and Davison.<sup>22</sup> Except for the resonance transition, however, the present results are not in harmony with the  $f$  values tabulated by Wiese *et al.*<sup>23</sup> These last oscillator strengths resulted from calculations that did not include the effect of core polarization either in the valence-electron Hamiltonian or in the dipole transition moment.

(b) *Potassium*. In Fig. 2 the calculated potassium photoionization cross section is compared with Hudson and Carter's measurement.<sup>20</sup> As with the sodium results, the agreement is good from threshold through the region of the cross-section minimum, but at smaller wavelengths the measured cross section rises much more steeply than the computed cross section does. The minimum values  $\sigma_{\text{min}}$  and  $\lambda_{\text{min}}$  computed for potassium are compared with the estimate of Seaton and with experimentally determined values in Table VIII. Again the overall agreement is very good.

The calculated values of the Fano parameter  $\chi$  are plotted in Fig. 3, together with the values of  $\chi$  determined by the experiment of Baum *et al.* The sensitivity of computed  $\chi$  values to the size of the core radius  $r_c$  is also illustrated. If the core-polarization correction to the dipole moment is neglected, the computed zero-point of  $\chi(E)$  is more than 0.5 eV greater than the measured zero point, and the computed photoionization cross-section minimum occurs at  $\lambda_{\text{min}} \sim 2475 \text{ \AA}$ , as opposed to the observed position  $\lambda_{\text{min}} \sim 2725 \text{ \AA}$ .

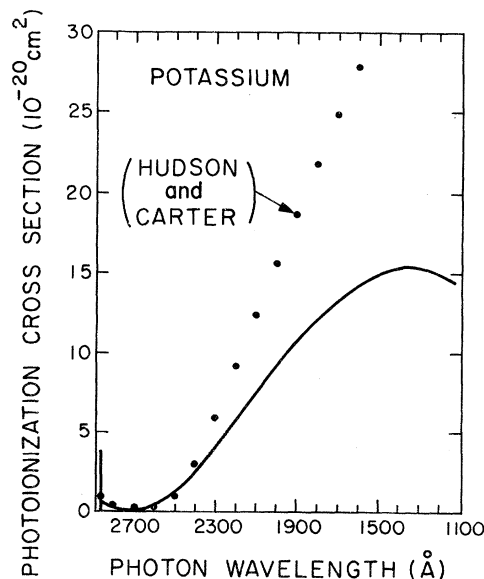


FIG. 2. Same as Fig. 1, for potassium. The filled circles are measurements reported by Hudson and Carter, Ref. 20.

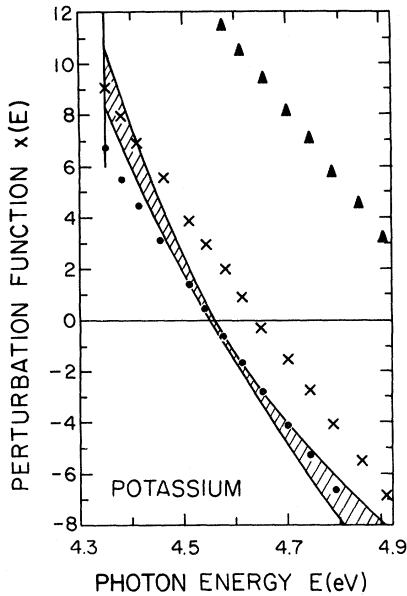


FIG. 3. Perturbation function  $x(E)$  for potassium. The filled circles are results obtained with  $r_c = 4.220a_0$ , the crosses are results obtained with  $r_c = 4.635a_0$ , and the triangles are results obtained by neglecting the core-polarization correction to the dipole transition moment. The shaded area represents the width of 1 standard deviation in the experimental determination of  $x$  by Baum *et al.*, Ref. 16.

Figure 4 shows the potassium transition moments  $M_3$  and  $M_1$ , defined in Eq. (19), in the region of the cross-section minimum. The moment  $M_*$ , computed by neglecting the spin-orbit perturbation of the continuum  $p$  orbital, and the analogously defined moments  $R_3$ ,  $R_1$ , and  $R_*$ , computed by neglecting the core-polarization correction [i. e.,  $Q(r) \rightarrow -r$ ], are also plotted. The behavior of the quantity  $R_3 - R_1$  in this region is approximately linear, as Fano assumed. The difference  $M_3 - M_1$ , the quantity actually used in the calculation of  $x(E)$ , behaves less linearly than  $R_3 - R_1$ , but this nonlinear behavior is not as pronounced for the heavier alkali metals as it is for potassium.

The K principal-series oscillator strengths reported in Table VII are in harmony with the  $f$  values given by Marr and Creek<sup>21</sup> and by Dalgarno and Davison,<sup>22</sup> but do not agree with the values suggested by Wiese *et al.*<sup>23</sup> Again, this is because these last  $f$  values are based on calculations that do not include any effect of core polarization.

(c) *Rubidium*. The rubidium photoionization cross section  $\sigma_T$ , computed with and without the core-polarization correction to the dipole transition moment, and the measurements by Marr and Creek<sup>18</sup> are shown in Fig. 5. The agreement between the experimental data and the "corrected" cross section is extremely good. The values of  $\lambda_{\min}$  and  $\sigma_{\min}$

computed for Rb are given in Table VIII and again the present results are consistent with the results of Seaton and of Marr and Creek.<sup>18</sup>

The values of  $x$  for rubidium that are listed in Table V and that have been determined by Baum *et al.* are plotted in Fig. 6. The calculated  $x$  values agree with the measured  $x$  values from the ionization threshold through the region of the cross-section minimum. However, for photon energies  $E > 5.2$  eV, the theoretical and experimental results for  $x(E)$  are not in harmony, in contrast with the over-all agreement for the photoionization cross section.

The computed Rb total oscillator strengths  $f_T = f_1 + f_3$  are in accord with the values suggested by Marr and Creek<sup>21</sup> since their  $f$  values are based on an extrapolation of the oscillator density  $df/d\epsilon$  determined from their photoionization cross-section measurements. For high-principal-series transitions, though, Dalgarno and Davison's recommended  $f$  values and the values of  $f_1$  and  $f_3$  computed by Warner<sup>24</sup> are not in good agreement with the present results, and the differences increase markedly with increasing principal quantum number.

(d) *Cesium*. Figure 7 shows the computed Cs photoionization cross section and Marr and Creek's measured cross section.<sup>18</sup> Throughout the range of photon energies considered, the ratio of the experi-

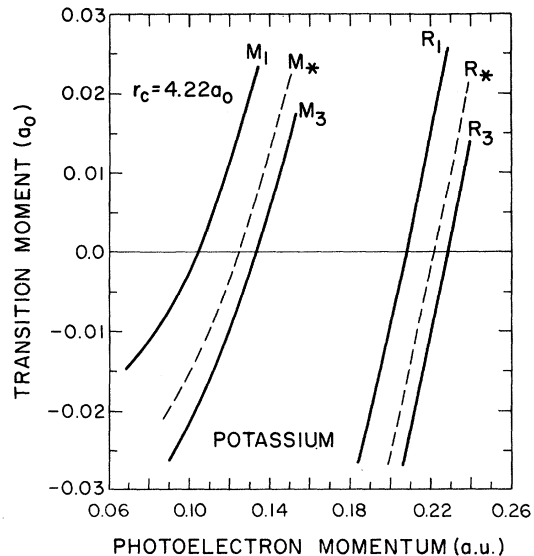


FIG. 4. Potassium transition moments for ground-state photoionization. The moments  $M$  include the core-polarization correction, while the moments  $R$  do not. Subscripts (1) and (3) refer to transitions to degenerate ( $j = \frac{1}{2}$ ) and ( $j = \frac{3}{2}$ ) continuum levels, and the subscript (\*) refers to moments computed by neglecting the spin-orbit perturbation of continuum  $p$  orbitals. When multiplied by  $(2/\pi k)^{1/2}$ , these bound-continuum moments join smoothly at the ionization threshold to bound-bound moments.

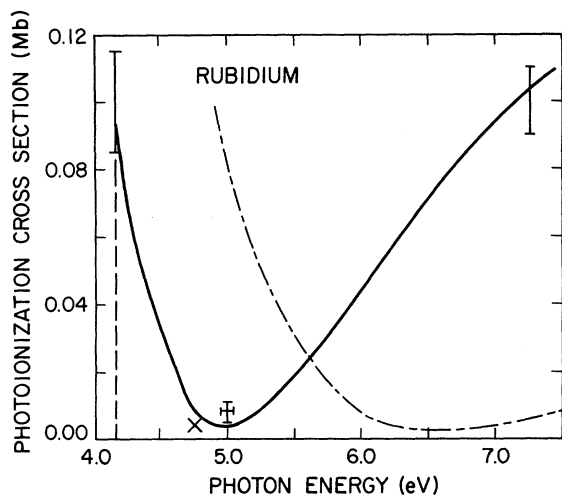


FIG. 5. Rubidium photoionization cross section ( $1 \text{ Mb} = 10^{-18} \text{ cm}^2$ ). The full curve and dashed curve indicate, respectively, results obtained with and without the core-polarization correction to the dipole transition moment. The bars indicate values measured by Marr and Creek, Ref. 18, and the cross indicates the cross-section minimum calculated by Seaton, Ref. 4.

mental results to the theoretical results is very nearly 2. The source of this large discrepancy is not established, but if the experimental data are in error it may be due to molecular Cs absorption: Creek and Marr<sup>25</sup> have reported the Cs molecular-

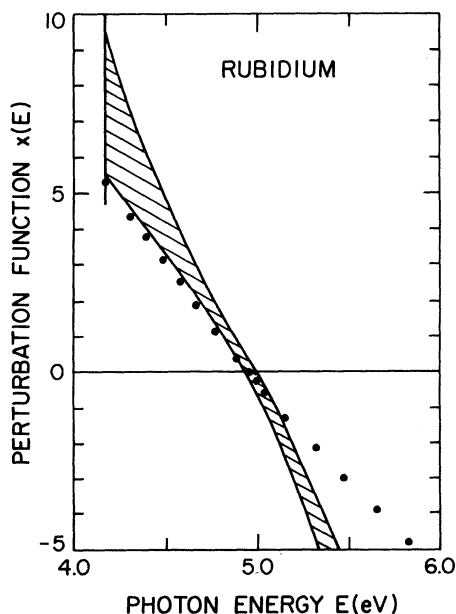


FIG. 6. Perturbation function  $x(E)$  for rubidium. The filled circles indicate values computed with  $r_c = 3.505a_0$ , and the shaded area indicates the width of 1 standard deviation in the experimental determination of  $x$  by Baum *et al.*, Ref. 16.

absorption cross section, in the region of the atomic Cs ionization threshold, to be as large as  $8 \times 10^{-18} \text{ cm}^2$  with an absolute uncertainty of  $\pm 50\%$ . This value is some 40 times greater than the cesium atomic photoionization cross section at threshold. The present computed value of  $\sigma_{\text{min}}$  is consistent with Seaton's estimate, and the computed value of  $\lambda_{\text{min}}$  is in good agreement with the position of the minimum given by Marr and Creek.<sup>18</sup> All of these values are listed in Table VIII.

As indicated earlier, the above Cs results were obtained with the core-radius value determined from measurements of photoelectron polarization,  $r_c = 4.834a_0$ , where  $a_0$  is the Bohr radius. Results obtained by using  $r_c = 6.100a_0$  are also given in Fig. 7. This  $r_c$  value reproduces the measured photoionization cross section at threshold. The resultant values of  $\lambda_{\text{min}}$  and  $\sigma_{\text{min}}$  clearly are not in harmony either with the calculation by Seaton or with the measurement by Marr and Creek.<sup>18</sup>

Further substantiation for the use of  $r_c = 4.834a_0$  in the calculations is given by the fact that there are two independent determinations of  $x(E)$ . Data from both experiments and computed results are plotted in Fig. 8. The values of  $x(E)$  calculated with  $r_c = 4.834a_0$  are in good agreement with the ex-

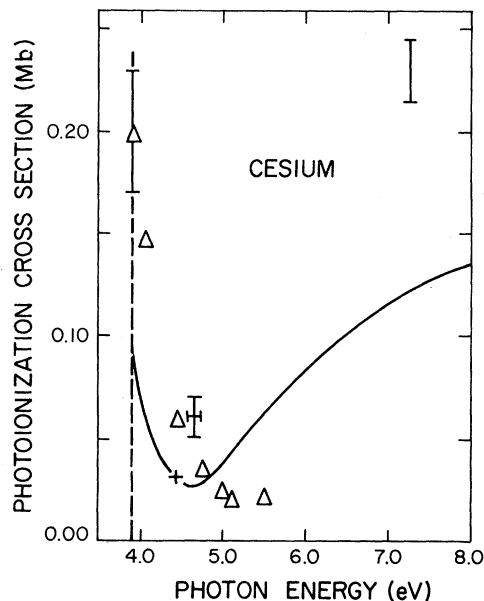


FIG. 7. Cesium photoionization cross section ( $1 \text{ Mb} = 10^{-18} \text{ cm}^2$ ). The full curve indicates results computed with  $r_c = 4.834a_0$ , the core-radius value obtained from the experimental determination of  $x(E)$ . The triangles indicate results computed with  $r_c = 6.100a_0$ , the core-radius value that yields agreement with the measured cross section at threshold. The bars indicate values measured by Marr and Creek, Ref. 18, and the cross indicates the cross-section minimum calculated by Seaton, Ref. 4.

perimental results. In particular, the zero point of  $x(E)$  appears to be well established in the neighborhood of  $E=4.52$  eV, but the use of  $r_c=6.100a_0$  yields a computed zero point of  $x(E)$  at  $E>5.20$  eV.

On the other hand, oscillator strengths computed with  $r_c=6.100a_0$  agree much better with  $f$  values reported by previous investigators<sup>15,21,24,26</sup> than do oscillator strengths computed with  $r_c=4.834a_0$ . The  $f$  values that are computed with  $r_c=4.834a_0$  (listed in Table VII) are consistently smaller, except for the resonance transition oscillator strengths  $f_1$  and  $f_3$ , than those calculated or measured by others. These comments are illustrated in Fig. 9, which shows ratios of selected  $f$  values to the  $f$  values given in Table VII.

In light of this disagreement, the neglected corrections to Eqs. (20)–(22) were examined. Neither of the corrections mentioned in Sec. II changed the computed zero point of  $x(E)$  by more than 0.05 eV.

There is an independent means of resolving the discrepancy between the measured oscillator strengths and photoionization cross section, and the oscillator strengths and photoionization cross section computed with  $r_c=4.834a_0$ , the core-radius value that reproduces the measured zero point of  $x(E)$ . Baum *et al.* noted that their polarization measurements indicate  $x=2$  below the cesium-ionization threshold. According to Eq. (20) this implies a pole in the  $^2P$  line-strength ratio  $\rho$ , and

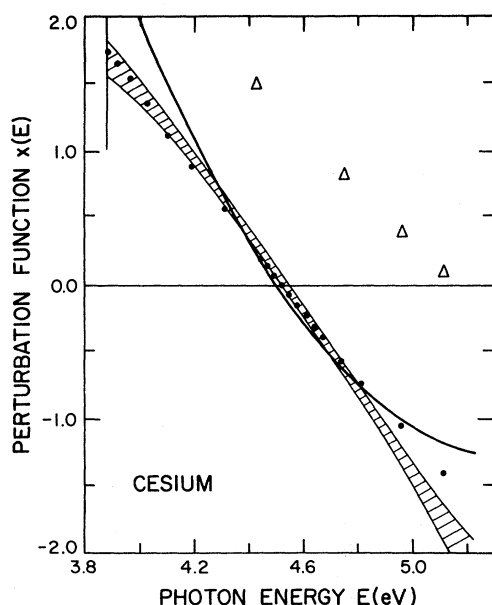


FIG. 8. Perturbation function  $x(E)$  for cesium. The filled circles and triangles are results computed with  $r_c=4.834a_0$  and  $r_c=6.100a_0$ , respectively. The shaded area indicates the width of 1 standard deviation in the experimental determination of  $x$  by Baum *et al.*, Ref. 16; the full curve indicates the quadratic least-squares fit by Kessler *et al.*, Ref. 17, to their experimental determination of  $x(E)$ .

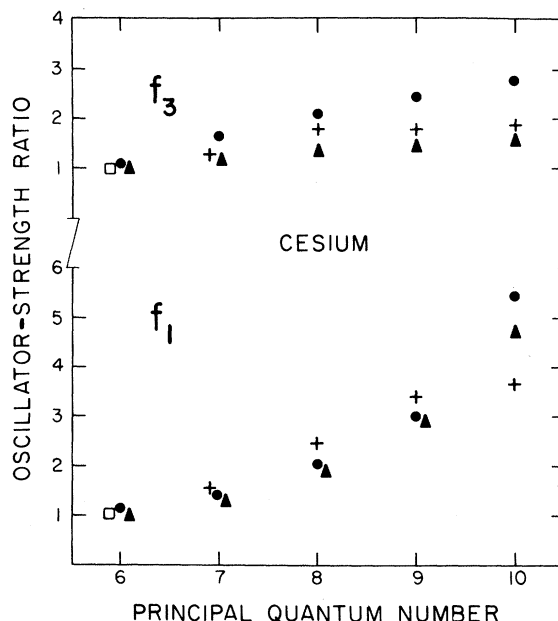


FIG. 9. Ratios of selected cesium oscillator strengths reported by other investigators to the  $f$  values listed in Table VII of this paper.  $f_1$  and  $f_3$  denote  $f$  values for transitions to  $(j=\frac{1}{2})$  and  $(j=\frac{3}{2})$   $^2P$  levels, respectively. The displayed data are from the following references: (□)—J. K. Kink, J. Opt. Soc. Am. 56, 1195 (1966); (+)—L. Agnew, Ref. 25; (●)—P. M. Stone, Ref. 15; (▲)—present investigation, but with  $r_c=6.100a_0$ .

Baum *et al.* searched the literature for confirmation of the existence of this pole. (See Ref. 16 for a complete bibliography.) Invariably the measured doublet line-strength ratio increases with increasing principal quantum number  $n$ , for  $n=6$  to  $n=10$ . However, for higher principal quantum numbers the results are conflicting: Some measurements of  $\rho$  indicate that a pole exists, while others indicate that a pole does not exist.

Our calculations with  $r_c=4.834a_0$  yield a pole very near the  $6s-16p$  transitions. Both the calculations with  $r_c=6.100a_0$ , the core-radius value that reproduces the measured photoionization cross section at threshold, and the experimental determination of  $x(E)$  by Kessler *et al.* indicate that  $x=2$  above the cesium-ionization threshold (see Fig. 8), and hence that no pole in the doublet line-strength ratio exists.

#### ACKNOWLEDGMENTS

The author wishes to thank Professor A. Dalgarno and Dr. D. Norcross for several informative conversations, and Professor W. Raith, Dr. G. Baum, Dr. M. Lubell, Professor J. Kessler, Dr. U. Heinzmann, and Dr. J. Lorenz for providing experimental results prior to publication. Professor Dalgarno is also thanked for a critical reading of the manuscript.

\*Work supported in part by National Aeronautics and Space Administration under Grant No. NGL 22-007-136.

- <sup>1</sup>I. B. Bersuker, *Opt. Spectry.* **3**, 97 (1957).  
<sup>2</sup>S. Hameed, A. Herzenberg, and M. G. James, *J. Phys. B* **1**, 882 (1968).  
<sup>3</sup>E. Fermi, *Z. Physik* **59**, 680 (1930).  
<sup>4</sup>M. J. Seaton, *Proc. Roy. Soc. (London)* **A208**, 418 (1951).  
<sup>5</sup>U. Fano, *Phys. Rev.* **178**, 131 (1969); **184**, 250 (1969).  
<sup>6</sup>G. McGinn, *J. Chem. Phys.* **50**, 1404 (1969).  
<sup>7</sup>T. Caves and A. Dalgarno (private communication).  
<sup>8</sup>C. J. Kleinman, Y. Hahn, and L. Spruch, *Phys. Rev.* **165**, 53 (1968); A. Dalgarno, G. F. W. Drake, and G. Victor, *ibid.* **176**, 194 (1968).  
<sup>9</sup>D. Norcross (private communication).  
<sup>10</sup>J. C. Weisheit and A. Dalgarno, *Chem. Phys. Letters* **9**, 517 (1971).  
<sup>11</sup>J. C. Weisheit and A. Dalgarno, *Phys. Rev. Letters* **27**, 701 (1971).  
<sup>12</sup>C. Bottcher, *J. Phys. B* **4**, 1140 (1971).  
<sup>13</sup>E. Clementi, *IBM J. Res. Develop. Suppl.* **9** (1965).  
<sup>14</sup>D. R. Hartree, *Proc. Roy. Soc. (London)* **A151**, 96 (1935); **A143**, 506 (1934).  
<sup>15</sup>P. M. Stone, *Phys. Rev.* **127**, 1151 (1962).  
<sup>16</sup>G. Baum, M. S. Lubell, and W. Raith, *Phys. Rev. Letters* **25**, 267 (1970); and private communication.  
<sup>17</sup>J. Kessler and J. Lorenz, *Phys. Rev. Letters* **24**, 87 (1970); U. Heinzmann, J. Kessler, and J. Lorenz (private communication).  
<sup>18</sup>G. V. Marr and D. M. Creek, *Proc. Roy. Soc. (London)* **A304**, 233 (1968).  
<sup>19</sup>R. D. Hudson and V. L. Carter, *J. Opt. Soc. Am.* **57**, 651 (1967).  
<sup>20</sup>R. D. Hudson and V. L. Carter, *Phys. Rev.* **139**, A1426 (1965).  
<sup>21</sup>G. V. Marr and D. M. Creek, *Proc. Roy. Soc. (London)* **A304**, 245 (1968).  
<sup>22</sup>A. Dalgarno and W. D. Davison, *Mol. Phys.* **13**, 479 (1967).  
<sup>23</sup>W. L. Wiese, M. W. Smith, and B. M. Glennon, *Atomic Transition Probabilities* (U. S. GPO, Washington, D. C., 1966).  
<sup>24</sup>B. Warner, *Monthly Notices Roy. Astron. Soc.* **139**, 115 (1968).  
<sup>25</sup>D. M. Creek and G. V. Marr, *J. Quant. Spectry. Radiative Transfer* **8**, 1431 (1968).  
<sup>26</sup>L. Agnew, *Bull. Am. Phys. Soc.* **11**, 327 (1966).

## Bremsstrahlung Rate and Spectra from a Hot Gas ( $Z = 1$ )\*

Stephen Maxon

*Lawrence Livermore Laboratory, University of California, Livermore, California 94550*

(Received 11 November 1971)

An interpolation between the quadrupole and extreme relativistic electron-electron bremsstrahlung contribution to the emission rate and spectra from a Maxwell-Boltzmann electron gas is carried out. These results are then added to the "exact" electron-ion results already in the literature to give the total emission for the temperature region  $1 \text{ keV} \leq kT_e \leq 0.3 \text{ MeV}$ . It is found that quadrupole corrections are sufficient until the temperatures reach  $kT_e \approx 100 \text{ keV}$ . At higher temperatures all multipoles must be included in order to describe the emission accurately.

### I. INTRODUCTION

In a previous publication,<sup>1</sup> the quadrupole electron-electron ( $e-e$ ) contribution to the bremsstrahlung spectrum of a hot Maxwell gas was given. It was found that sizable corrections to the short-wavelength portion of the spectrum occur when  $kT_e \gtrsim 20 \text{ keV}$ . There also exists in the literature an integration of the Bethe-Heitler cross-section for electron-ion ( $e-i$ ) bremsstrahlung over a relativistic Maxwell-Boltzmann distribution of electrons.<sup>2</sup> A simple formula<sup>3</sup> was given for including corrections to the well-known dipole spectrum. For  $e-i$  bremsstrahlung, successively higher-order multipoles will be down by a factor  $kT_e/mc^2$  from the previous order, whereas the factor will be  $(kT_e/mc^2)^2$  for  $e-e$  bremsstrahlung, since only the  $2^{2n}$  ( $n = 1, 2, \dots$ ) poles contribute.

One of the important applications of this work

is in the field of observational x-ray astronomy. It is standard practice, nowadays, to fit the spectrum of an x-ray source with a black body, thermal bremsstrahlung, or synchrotron model and thereby determine the electron temperature from the data. In this way a temperature of  $8.1 \times 10^7 \text{ K}$  (7 keV) was measured for SCO X-1<sup>4</sup> and a temperature of  $3.5 \times 10^8 \text{ K}$  (30 keV) was measured for CYG X-1.<sup>5</sup> Measurements also show a strong variation in intensity over periods ranging from fractions of a second to months.

In this paper, an interpolation between the quadrupole and extreme relativistic  $e-e$  bremsstrahlung rate and spectra is carried out.

In Sec. II the method of interpolation is discussed and graphs of the  $e-e$  spectra are given for several different temperatures. In Sec. III, the  $e-e$  and  $e-i$  contributions are added together to obtain the total bremsstrahlung spectra and rate over the